MRR and chip formation during turning T6 tempered Al 7075 alloy: An Experimental investigation

SANTOSH KUMAR BARAL,Raajdhani Engineering College, Bhubaneswar
SMRUTIREKHA GIRI,Aryan Institute of Engineering and Technology, Bhubaneswar
RAMYARANJAN LENKA,NM Institute of Engineering and Technology, Bhubaneswar
Mr. DEBANANDA BEHERA,Capital Engineering College, Bhubaneswar

Abstract

Aluminium 7075 alloy is a suitable material for applications in automobile and aerospace industry for its light weight, excellent mechanical properties and castability. Most of the casting components need some sort of machining for the finishing. Here in this literature studies have been conducted on metal removal rate of Al 7075 alloy and chip formation. This analysis will help in calculating machining time, cost of machining and surface roughness of machined components. The aluminium alloy considered is T6 tempered which is used in most of the automobile and aerospace applications.

Keywords: Al 7075; Turning; Material removal rate; Chip reduction coefficient; Chips

1. Introduction

Al 7075 is a Zn-Mg-Cu base aluminium alloy possessing high strength, moderate toughness and corrosion resistance. It is commonly used for structural applications in aircraft and aerospace industries. Previously copper based Al 2xxx series of alloys were the most common aerospace alloys, but they were susceptible to stress corrosion cracking. However, presence of chromium as an alloying element adds the benefit of stress-corrosion cracking resistance in Al 7075 and hence it is replacing the Al 2xxx series of alloys in many critical applications [1].

While producing thinner chips during high speed machining of Al 7075-T6 alloy, the chip flow angle and shear angle became high; but the thrust forces were low [2]. The life of polycrystalline diamond (PCD) tools was better than the carbide tools during high speed turning of Al 7075 alloy in dry condition [3]. During ultra-high speed machining Al-Mg alloy with tungsten carbide tool, Yousefi and Ichida [4] observed lower surface roughness values at higher cutting speed; and the minimum value was attended at 260 m/min. Diamond inserts exhibited excellent performance in terms of tool wear while ultra-high precision machining (UHPM) of RSA 905 (a modified grade of Al 6061); and abrasion was the dominant mechanism of tool wear [5]. While turning Al-Cu based UNS A92024 and Al-Zn based UNS A97050 in dry condition with uncoated and titanium nitride coated tungsten carbide inserts, Gomez-Parra et al. [6] reported the Built-Up-Edge (BUE) was formed by mechanical adhesion, whereas thermo- mechanical reasons formed Built-Up-Layer (BUL) primarily. As a result of the extrusion of the BUE, a secondary BUL was formed. The tool position angle was changed by BUE which resulted reduced values of surface roughness. Yusuf et al. [7] observed different shapes of chips while machining LM6 and Al 7075 alloy under similar cutting conditions. During drilling ACP 5080 aluminium alloy with high speed steel twist drills, Kelly and Cotterell [8] observed snarled ribbon chips in dry machining condition, a combination of loose arc and short conical chips in mist and compressed air lubrication; and loose arc chips in flood lubrication.

Though wide research has been conducted to investigate the influence of different machining process parameters on tool wear and surface quality of Al 7075 alloy, investigation on material removal rate, chip forms and chip reduction coefficient is limited. Moreover, use of cutting fluids during machining improve machinability; however, these seriously degrade environmental quality. But dry machining is a challenge, particularly in aerospace engineering [9]. Accordingly, this paper presents a systematic study of the above lacking and challenging area during turning the Al 7075 alloy with uncoated tungsten carbide tools in dry environment.

2. Materials and methods

T6 tempered Al 7075 alloy (supplied by Bharat Aerospace Metals, Mumbai) was used as workpiece for the turning

experiments. Chemical composition test result of the alloy is presented in Table 1. The workpiece was of length 200 mm and 50 mm diameter; and it was machined for a length of 150 mm using a high speed precision lathe of make and model HMT-NH 22 (maximum power and spindle speed of 11 kW and 2040 rpm respectively) in dry condition. Uncoated tungsten carbide inserts of ISO specification CNMG 120408 mounted securely to PCLNR 2525M 12 turning tool holder were used for chip removal during turning. The experimental setup during turning is shown in Fig. 1. Lathe spindle speed, feed and depth of cut were the three process parameters during turning and four levels were assigned to each parameter, which are presented in Table 2. Experiments were conducted following Taguchi L_{16} Design of Experiments (DOE). Weight of the workpiece was measured before and after each run by a Satwik-VIK03HL weighing scale of maximum capacity 3 kg and least count 100 mg. Eq. (1) was used to calculate material removal rate during each run and analyzed. Thickness of chips formed during turning was measured using Mitutoyo Absolute Digimatic vernier caliper. Chip reduction coefficient (Z) was determined using Eq. (2) and analyzed.

$$MRR(mm^3/\min) = \frac{W_L * f * N}{\rho * L_m} \quad (1)$$

$$Z = \frac{a_2}{a_1} \quad (2)$$

where, W_L = weight loss (g) in the machined sample, ρ = density of the T6 tempered Al 7075 alloy, which is assumed as 0. 00281 g/mm^3 [10], L_m = length (mm) of machining, a_1 = thickness (mm) of uncut layer of chips = $f * sin(\varphi)$, φ = principal cutting angle of the tool, i.e. 95^0 for the turning tool holders of geometry PCLNR 2525M 12 [11], a_2 = measured thickness (mm) of the chips formed.

Table 1 Result of chemical composition test

Element	Ti	Si	Mn	Fe	Cr	Cu	Mg	Zn	Al
Weight %	0.04	0.10	0.12	0.21	0.24	1.50	2.00	4.60	Rest

Table 2 Turning process parameters and their levels

Parameters	Levels of parameters			
	1	2	3	4
Spindle speed, N (rpm)	250	715	1210	1575
Feed, f (mm/rev)	0.05	0.1	0.16	0.2
Depth of cut, d (mm)	0.2	0.3	0.4	0.5

Fig. 1 Experimental setup during turning the Al 7075 alloy

3. Results and discussion

Experimental results for MRR and Z during turning the alloy following Taguchi L_{16} DOE, with uncoated tungsten carbide inserts are presented in Table 3. Minimum amount of material (260.97 mm^3/min) was removed at the lowest levels of spindle speed, feed and depth of cut (run 1). It increased to 15170.82 mm^3/min (run no. 16) while turning at the highest levels of speed and feed at the same depth of cut (0.2 mm). While turning at constant spindle speed with

increasing feed and depth of cut (run no. 1-4), the MRR increased. Moreover, while turning the alloy at constant speed and increasing feed, a significant increase in the MRR was observed even though the depth of cut was reducing consistently (run 13-16). Similarly, minimum value of Z (1.044) was achieved for run no. 16, i.e. while machining at 1575 rpm of spindle speed, 0.2 mm/rev of feed and 0.2 mm of depth of cut. Experimental results (run 1-4) reveal that Z increased on increasing feed along with depth of cut at constant spindle speed. From the results of runs 13-16, it is observed that while turning the alloy at constant spindle speed, Z reduced with the reduction of depth of cut and increase in feed.

Signal-to-Noise (SN) ratios for MRR and Z were determined considering "larger is better" criteria and "smaller is better" criteria respectively; and are presented in Table 3. Response table (Table 4) and main effects plot (Fig. 2) for SN ratios of MRR reveal that the mean SN ratio of MRR increased with increase in spindle speed, feed and depth of cut. Mean SN ratios were maximum for fourth levels of machining process parameters (N_4-f_4-d_4), i.e. 1575 rpm of spindle speed, 0.2 mm/rev of feed and 0.5 mm of depth of cut. This was the optimal combination of machining process parameters [12] for MRR, while turning the Al 7075 alloy with uncoated tungsten carbide inserts in dry environment. Response table (Table 5) and main effects plot (Fig. 3) for SN ratios of Z reveal that the mean SN ratio of Z increased on increasing spindle speed, but reduced on increasing depth of cut. Maximum values of mean SN ratio were obtained for N_4-f_4-d_1, i.e. spindle speed 1575 rpm, feed 0.2 mm/rev and depth of cut 0.2 mm. This was the optimal combination of machining parameters for Z, while turning the Al 7075 alloy with uncoated tungsten carbide inserts in dry environment.

To verify the improvement of performance characteristics, some confirmatory experiments were conducted and the results are presented in Table 6. Closeness between the predicted and experimental values observed; and the improvement of SN ratio for optimal parameters was 9.156 dB for MRR and 7.635 dB for Z. ANOVA results at 95% confidence level (Table 7 for MRR and Table 8 for Z) revealed that for MRR, spindle speed was the most significant parameter, taken after by feed; and the influence of depth of cut was not significant. Similarly the most significant parameter for Z was depth of cut, taken after by spindle speed; and the influence of feed was not significant.

Table 3 Experimental results for MRR and Z during turning the alloy

Run No.	N	f	d	W_L (g)	MRR (mm^3/min)	a_1 (mm)	a_2 (mm)	Z
1	250	0.05	0.2	8.8	260.97	0.050	0.103	2.315
2	250	0.1	0.3	18.7	1109.13	0.100	0.273	2.744
3	250	0.16	0.4	26.2	2486.36	0.159	0.510	3.200
4	250	0.2	0.5	28.7	3404.51	0.199	0.643	4.729
5	715	0.05	0.3	21.3	1806.58	0.050	0.174	2.498
6	715	0.1	0.2	17.2	2917.67	0.100	0.173	2.340
7	715	0.16	0.5	45.9	12457.79	0.159	0.327	3.853
8	715	0.2	0.4	26.9	9126.22	0.199	0.280	3.105
9	1210	0.05	0.4	27.2	3904.15	0.050	0.157	2.444
10	1210	0.1	0.5	33.8	9702.97	0.100	0.290	2.906
11	1210	0.16	0.2	19.5	8956.58	0.159	0.303	1.700
12	1210	0.2	0.3	14.3	8210.20	0.199	0.173	2.287
13	1575	0.05	0.5	36.1	6744.66	0.050	0.133	2.677
14	1575	0.1	0.4	30.6	11434.16	0.100	0.177	2.173
15	1575	0.16	0.3	25.1	15006.41	0.159	0.221	1.884
16	1575	0.2	0.2	20.3	15170.82	0.199	0.220	1.044

Table 4 Response table for SNR of MRR

Table 5 Response table for SNR of Z

SNR MRR (dB)	SNR Z (dB)
48.332	-7.289
60.900	-8.767
67.911	-10.102
70.641	-13.495
65.137	-7.951
69.301	-7.384
81.909	-11.717
79.206	-9.842
71.831	-7.761
79.738	-9.266
79.043	-4.611
78.287	-7.185
76.579	-8.552
81.164	-6.743
83.526	-5.502
83.620	-0.376

Level	N	f	d
1	61.95	65.47	70.07
2	73.89	72.78	71.96
3	77.22	78.1	75.03
4	81.22	77.94	77.22
Delta	19.28	12.63	7.14
Rank	1	2	3
Level	N	f	d
1	-9.913	-7.889	-4.915
2	-9.224	-8.04	-7.351
3	-7.206	-7.983	-8.612
4	-5.293	-7.725	-10.758
Delta	4.620	0.315	5.843

Rank	2	3	1

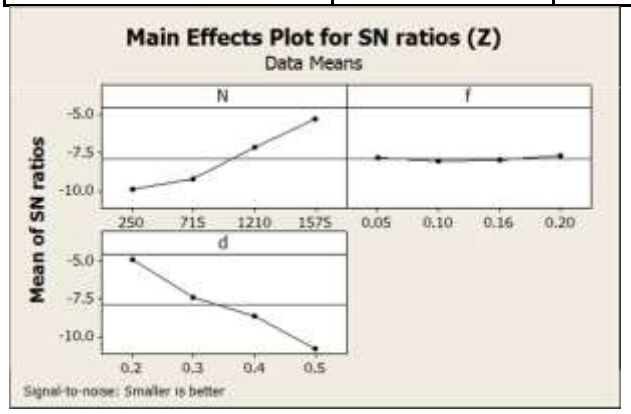

Fig. 2 Main effects plot for SNR of MRR

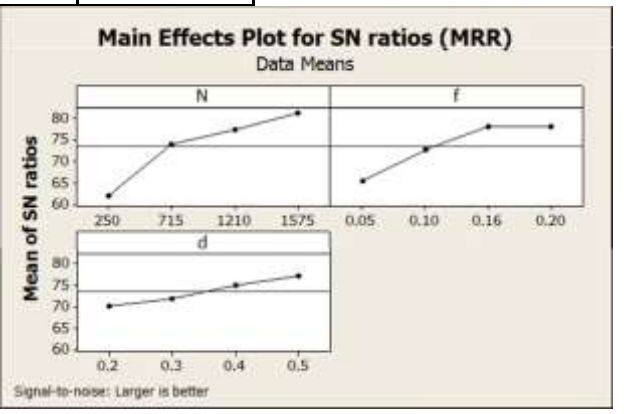

Fig. 3 Main effects plot for SNR of Z

Table 6 Confirmation test results

	Initial machining parameters	Optimal machining parameters			
		Prediction	Experiment	Prediction	Experiment
Level	N_2-f_2-d_2	N_4-f_4-d_4	N_4-f_4-d_4	N_4-f_4-d_1	N_4-f_4-d_1
MRR	5349.76		15349.62		
Z	2.515				1.044
SN Ratio (dB) for MRR	74.566	89.237	83.722		
SN Ratio (dB) for Z	-8.796			-2.115	-0.376
Improvement of SN ratios		9.156 dB for MRR and 7.635 dB for Z			

Table 7 ANOVA for MRR

Source	DF	SS	MS	F	P
N	3	213727576	71242525	11.04	0.007
f	3	105767928	35255976	5.46	0.038
d	3	5880912	1960304	0.3	0.822
Error	6	38730482	6455080		
Total	15	364106899			

Table 8 ANOVA for Z

Source	DF	SS	MS	F	P
N	3	4.155	1.3851	14.88	0.003
f	3	0.224	0.0745	0.8	0.537
d	3	6.102	2.0339	21.85	0.001
Error	6	0.558	0.0931		
Total	15	11.039			

Linear regression models were developed for both MRR and Z using the corresponding experimental results from

Table 3, through MINITAB 16 software; and these are presented in Eqs. (3) and (4) respectively. High determination coefficients (R^2) of both the models (81.16% for MRR and 92.84% for Z) and their reasonable agreement with the corresponding adjusted R^2 values justify their adequacy and fitness to the sample data. Moreover, the residuals are distributed closely to the normal probability lines in the normal probability plots of residuals (Figs. 4 and 5), which reveal significancy and adequacy of the models.

$$MRR = -6311.58 + 7.07186N + 41884.4f + 3957.55d \quad (3)$$

$R^2 = 81.16\%$, $R^2(adj) = 76.44\%$

$$Z = 1.39887 - 0.00100965N + 2.02511f + 5.4519d \quad (4)$$

$R^2 = 92.84\%$, $R^2(adj) = 91.05\%$

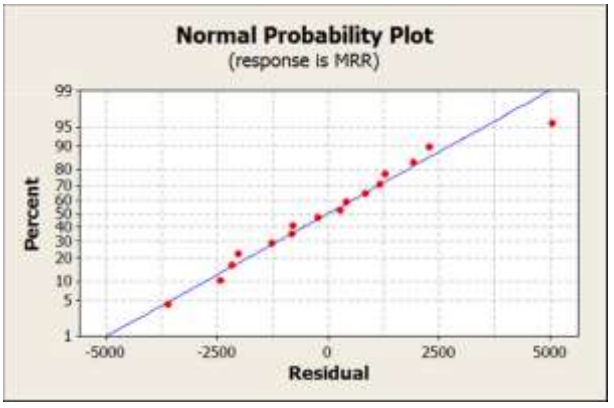

Fig. 4 Normal probability plot for MRR

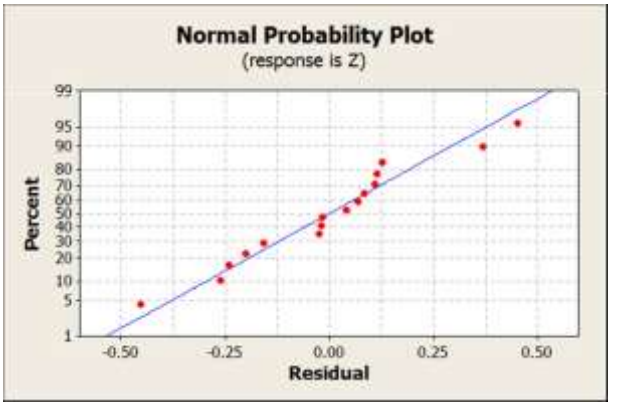

Fig. 5 Normal probability plot for Z

Photographic images of the chips formed during turning the alloy are presented in Fig. 6 (a-p). Spring type, tubular, continuous and close coiled helical chips (Fig. 6 a-b) were observed at low levels of machining parameters; but these became open coiled helical and near to spiral (Fig. 6 c-d) on increasing feed and depth of cut. With the increase of spindle speed, the chips were continuous and flat (Fig. 6 e-f) at lower levels of feed and depth of cut; and on increasing the feed and depth of cut, the chips became spiral in shape (Fig. 6 g-h). Long, continuous and ribbon- like spiral chips were formed at higher level of spindle speed (1210 rpm). However, at this speed level, short and saw-toothed chips (Fig. 6 j) were observed at feed 0.1 mm/rev and depth of cut 0.5 mm. High speed (1575 rpm) machining produced discontinuous, short and saw-toothed curled chips (Fig. 6 m-p) at different levels of feed and depth of cut, which was the favorable machining condition for high MRR and hence increased productivity.

(a)

(b)

(c)

(d)

(e) (f) (g) (h)

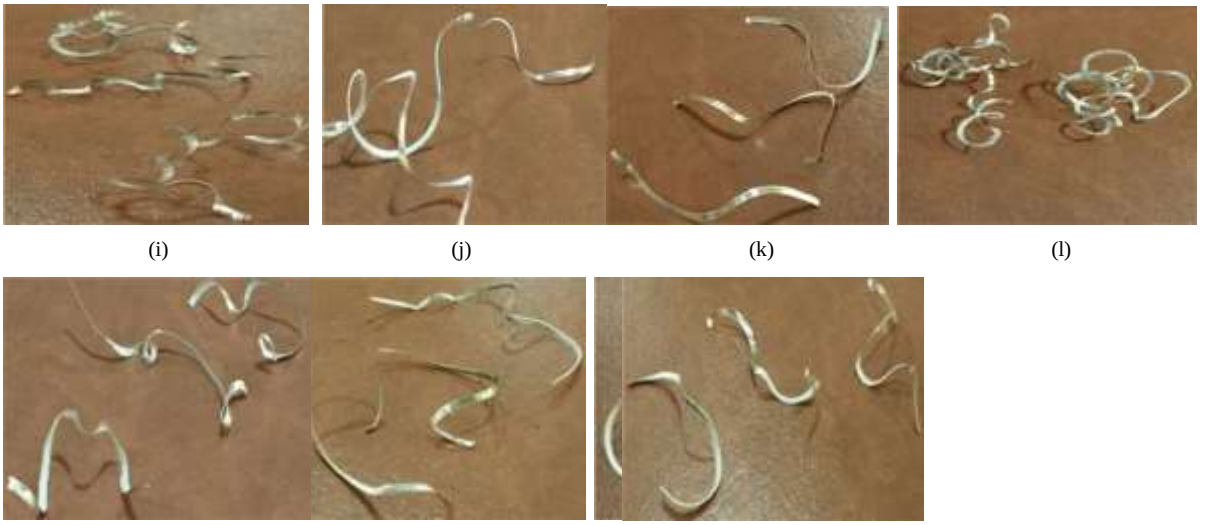

(i) (j) (k) (l)

(m) (n) (o) (p)

Fig. 6 Chip forms during turning the T6 tempered Al 7075 alloy at (a) run 1; (b) run 2; (c) run 3; (d) run 4; (e) run 5; (f) run 6; (g) run 7; (h) run 8; (i) run 9; (j) run 10; (k) run 11; (l) run 12; (m) run 13; (n) run 14; (o) run 15; and (p) run 16

4. Conclusion

- During turning T6 tampered Al 7075 alloy with uncoated tungsten carbide inserts in dry condition, the MRR increased with increasing any of the machining parameters. However, Z reduced on increasing lathe spindle speed and increased on increasing the depth of cut. The optimized machining process parameters for MRR was 1575 rpm of spindle speed, 0.2 mm/rev of feed and 0.5 mm of depth of cut; and that for Z was 1575 rpm of spindle speed, 0.2 mm/rev of feed and 0.2 mm of depth of cut.
- ANOVA results at 95% confidence level revealed that for MRR, spindle speed was the most significant parameter, taken after by feed; and the influence of depth of cut was not significant. Similarly the most significant parameter for Z was depth of cut, taken after by spindle speed; and the influence of feed was not significant. Linear regression models were developed for both the responses and their adequacy were verified.
- Spring type, tubular, continuous and close coiled helical chips were observed at low levels of machining parameters; but these became open coiled helical and near to spiral on increasing feed and cutting depth. With the increase of spindle speed, the chips were continuous and flat at lower levels of feed and cutting depth; and on increasing these parameters, the chips became spiral in shape. Long, continuous and ribbon-like spiral chips were formed at higher level of spindle speed (1210 rpm). However, at this speed level, short and saw- toothed chips were observed at feed 0.1 mm/rev and depth of cut 0.5 mm. High speed machining produced discontinuous, short and saw-toothed curled chips at various levels of feed and cutting depth.

References

[1] https://www.alcoa.com/mill_products/catalog/pdf/alloy7075techsheet.pdf, Alloy 7075 plate and sheet, ALCOA Mill Products
[2] http://www.sme.org/ProductDetail.aspx?id=17108&terms=high-speed%20machining%20of%207075, High Speed Machining of Aluminum 7075-T6
[3] A. Choudhary and S.R. Chauhan, Int. J. Machining and Machinability of Materials 13:1 (2013) 17-33.
[4] R. Yousefi and Y. Ichida, Precision engineering 24:4 (2000) 371–376.
[5] E.I.K. Hossein, O. Olufayo and Z. Mkoko, Wear 302:1-2 (2013) 1105-1112.
[6] A. Gomez-Parra, M. Alvarez-Alcon, J. Salguero, M. Batista and M. Marcos, Wear 302:1-2 (2012) 1209-1218
[7] M. Yusuf, M.K.A. Ariffin, N. Ismail and S. Sulaiman, Advanced Science Letters 19:4 (2013) 2243-2346
[8] J.F. Kelly and M.G. Cotterell, Journal of Materials Processing Technology 120 (2002) 327–334.
[9] M. Nouari, G. List, F. Girot and D. Coupard, Wear 255 (2003) 1359–1368.
[10] http://asm.matweb.com/search/SpecificMaterial.asp?bassnum=MA7075T6
[11] http://www.sandvik.coromant.com/en-gb/products/Pages/productdetails.aspx?c=pclnr+2525m+12
[12] D.S.C. Kishore, K.P. Rao and A. Ramesh, Materials Today: Proceedings 2 (2015) 3075-3083.